

# An Optimal Control Approach to Terminal Area Air Traffic Control

David K. Schmidt\* and Robert L. Swaim†  
*Purdue University, West Lafayette, Ind.*

In this investigation, the problem addressed is the specification of the curved approach paths and landing sequence for a group of aircraft desiring to land in a terminal area such that the terminal-area system performance is maximized. The multiple-aircraft problem includes the aspect of competition or cooperation between the vehicles by formulating the problem as a set of disconnected optimal trajectories. The flight paths are governed by kinematic equations of motion while in-flight and terminal-time separation inequality constraints between trajectories are imposed. The performance criterion for the system is the sum of the flight durations plus the integrated weighted accelerations of the aircraft. The solution approach employs penalty functions for the treatment of the inequality constraints and is based on the steepest descent algorithm. A number of examples are presented which involve interactions between two and three aircraft. Parametric results are also included for some single-aircraft examples. The basic approach assumes the initial conditions are known for all aircraft before the solution process begins. In addition, a sequential solution algorithm is also demonstrated which allows the initial conditions to be made known to the system only a short time before arrival into the terminal area. A comparison between the two algorithms is presented.

## Introduction

AIR traffic congestion is quite understandably prevalent in the terminal area and is expected to get worse in the future as predictions indicate that a four-fold increase in the number of terminal operations (takeoffs and landings) can be expected by 1995. Consequently, the FAA<sup>1</sup> is developing and incorporating new traffic control equipment into the ATC system such as the new microwave landing system (MLS). This MLS will not only provide better accuracy for standard approach procedures, but, when considered along with the new area navigation (RNAV) concepts, could also potentially provide greater freedom of trajectory selection for terminal area operations. The objective of this paper is, therefore, to summarize some of the results obtained (c.f. Ref. 2) concerning the application of optimal control techniques to the determination of the aircraft landing sequence and curved approach flight paths which are to improve terminal area system performance by making use of the flexibility provided by the new MLS and RNAV systems.

Within the topic of analytical investigations of terminal area traffic control, the approaches encountered range from operations research techniques to optimal control applications which are usually formulated as single aircraft, four dimensional guidance problems. Blumstein<sup>3</sup> and Simpson<sup>4</sup> were among the first to address the terminal area problem analytically by using queueing theory and simulation models to define maximum airport capacity and to make recommendations for new operational procedures. These procedures were variations of the techniques presently used such as holding queues, or "stacks" and one-dimensional instrument landing systems (ILS). These investigations pointed out the detrimental effect on capacity resulting from mixed traffic categories and common flight paths, particularly on the final ILS flight path. The advantages of curved approaches were implicit in

their suggestions to minimize the length of common final glide slopes.

Telson,<sup>5</sup> Athans and Porter,<sup>6</sup> and Tobias<sup>7</sup> addressed the problem of on-line algorithms for flow control. The flight paths were defined in a discrete manner such as constant-radius turns and straight-line segments. Complete freedom of flight-path geometry was not allowed and conflicts were eliminated by delaying the aircraft in holding patterns. Straight-line paths were specified between the intersection nodes in modeling the terminal area. Using this model, Telson and Athans and Porter assumed a single category of aircraft while Tobias made the similar assumption initially, then showed a capacity reduction of approximately 40% if two speed categories are assumed. These findings again show the potential advantage of complete freedom of flight-path selection and curved approaches for delivering aircraft with different velocity characteristics to the final landing gate.

Similar flight-path geometries are also present in the guidance approaches of Cherry, et al.,<sup>8</sup> Erzberger and Lee,<sup>9</sup> and Lee and McLean.<sup>10</sup> However, the freedom to select the flight path is provided for by a four-dimensional guidance technique to deliver the aircraft to a particular position and heading at a prescribed time. This guidance problem is, however, inherently single-aircraft oriented and the aspect of "competition" between aircraft is assumed to be incorporated in some higher level controller which specifies the final positions, velocities, and times.

Flight-path optimization of a single aircraft has been investigated quite extensively from the standpoint of maximizing the capability of the aircraft. Such problems as minimum-fuel trajectories or minimum-time trajectories to climb to altitude have been addressed. However, these investigations were not for the purpose of improving multiple-aircraft operations. Multiple-aircraft control, however, was investigated by Shultz and Kilpatrick<sup>11</sup> for an aircraft carrier landing system. Optimal-trajectory segments, such as minimum-fuel landing trajectories for a single aircraft, were used as portions of an overall control algorithm. The handling of conflicts, however, were heuristically controlled and the aircraft were all fighter-type aircraft with similar velocity characteristics.

In contrast to these investigations, this paper presents the multiple-aircraft landing problem formulated as a set of disconnected optimal trajectories.<sup>12,13</sup> This approach provides for three-dimensional, curved trajectories and includes the effect of "competition" between aircraft of var-

Received October 13, 1972; revision received January 2, 1973.

Index categories: Air Navigation, Communication and Traffic Control Systems; Navigation, Control, and Guidance Theory.

\*Ph.D. Candidate, School of Aeronautics, Astronautics, and Engineering Sciences; presently Visiting Assistant Professor. Member AIAA.

†Associate Professor. Associate Fellow AIAA.

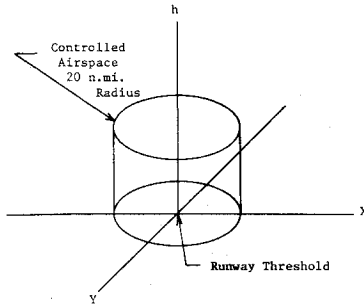


Fig. 1 Terminal area geometry.

ious flight characteristics. The solutions to some example problems are found via the Steepest-Descent technique.<sup>14</sup> Although preliminary in nature, this analysis is intended as a basic step toward the ultimate goal of optimal or semioptimal automated terminal air traffic control. The purpose is twofold. The first is to develop a unified optimal-control formulation of the ATC functions of landing sequencing, trajectory specification and aircraft spacing. The second is then to use this formulation and solution technique to develop, analyze, and compare various simpler semioptimal control policies which could be used, along with precomputed trajectories, by a computer controller for efficient, on-line air traffic control.

### Problem Definition and Formulation

Consider a number of aircraft desiring to land on a given runway available only to landing aircraft. These aircraft are assumed to be under positive control in the terminal airspace out to, say, 20 naut miles from the runway threshold, the origin of a ground based coordinate system as shown in Fig. 1. This terminal area system therefore consists of the aircraft subsystems over which direct flight-path control is possible. We then state the terminal-area-control problem as the determination of the aircraft trajectories such that some measure of total system performance is maximized (minimized). Constraints on the system include the differential equations of motion of the aircraft as well as in-flight and landing-time separation requirements.

This problem can be formulated as the determination of the optimal set of disconnected trajectories, depicted schematically in Fig. 2. Associated with each trajectory will be its equations of motion relating the  $n$  state variables,  $\bar{x}$ , and the  $m$  control variables,  $\bar{u}$ , of each aircraft.

$$i = 1, \dots, N$$

$$\bar{x}_i = \bar{f}_i(\bar{x}_i, \bar{u}_i, t) \quad t_{a_i} \leq t \leq t_{b_i} \quad (1)$$

These are the selected equations of motion of the  $i$ th aircraft while  $N$  is the total number of aircraft being considered. The aircraft's initial conditions are those at the time the aircraft enters the system (e.g. at 20 naut miles) and the terminal conditions are the selected final-approach conditions for that aircraft. Minimum in-flight separation constraints appear as state variable inequality constraints between aircraft such as

$$S(\bar{x}_i, \bar{x}_j) = \frac{(X_i - X_j)^2 + (Y_i - Y_j)^2}{R_{\min}^2} + \frac{(h_i - h_j)^2}{\Delta h_{\min}^2} \geq 1 \quad (2)$$

where  $X$ ,  $Y$ , and  $h$  are the aircraft position coordinates and  $R_{\min}$  and  $\Delta h_{\min}$  are the minimum allowable range and altitude separation, respectively. In the examples discussed later,  $R_{\min}$  and  $\Delta h_{\min}$  are 1.5 naut miles and 1000 ft, respectively.

Minimum time separation between aircraft arrivals at the final gate is obtained with the terminal constraint

$$T(t_i, t_j) = |t_{b_i} - t_{b_j}| - \Delta t_{\min} \geq 0 \quad (3)$$

where  $t_b$  is the final time for the aircraft and  $\Delta t_{\min}$  is the minimum time separation. This constraint is not used to determine the landing sequence as this could be determined from the unconstrained solution first.

The system performance index to be minimized consists of the sum of the aircraft flight times plus the weighted sum of the integrated aircraft accelerations. Or

$$\phi = \sum_{i=1}^N \{ (t_{b_i} - t_{a_i}) + \int_{t_{a_i}}^{t_{b_i}} (\bar{a}_i' W_{a_i} \bar{a}_i) dt \} \quad (4)$$

where  $(\bar{a}_i' W_{a_i} \bar{a}_i)$  is a quadratic form in terms of the weighted acceleration vector,  $\bar{a}_i$ , of the  $i$ th aircraft, while  $t_{a_i}$  and  $t_{b_i}$  are the entry time and final time of the  $i$ th aircraft. The first term tends to maximize aircraft landing flow while the second tends to maximize passenger comfort and provide for smooth trajectories.

It should be emphasized that the optimal-control problem here addresses the multiple-aircraft problem. The purpose is not to minimize the time for a particular aircraft, but a system of aircraft. In addition, there is a penalty for extreme aircraft acceleration which would not only be unpleasant for the passengers, but also difficult or impossible to achieve.

The final solution desired is the set of positions and velocities which the aircraft are to follow and not necessarily the aircraft controls (e.g., thrust, angle of attack, etc.). Hence, kinematic relationships only are needed. Additional constraints resulting from the performance capability of the vehicle, should they occur, would then impose flight path constraints. However, this would be done only after considering the unconstrained solution first, which is the subject of this investigation. With adequate weighting of the acceleration components in the performance index, little or no limitations on maneuverability may result.

The equations of motion to be used for the aircraft then consist of the kinematic equations

$$\dot{V} = a_v \quad \dot{\gamma} = a_\gamma / V$$

$$\dot{\chi} = a_\chi / V \cos \gamma \quad \dot{h} = V \sin \gamma \quad \dot{X} = V \cos \gamma \cos \chi$$

$$\dot{Y} = V \cos \gamma \sin \chi \quad (5)$$

where, as shown in Fig. 1,  $X$ ,  $Y$ , and  $h$  are the position coordinates with reference to a fixed, ground-based coordinate system with the origin at the landing runway threshold. Likewise,  $V$  is the aircraft velocity,  $\gamma$  the flight-path angle measured from the local horizon and  $\chi$  the heading angle measured from the positive  $X$  axis. The three controls are the accelerations in the velocity coordinate system. They consist of the longitudinal acceleration,

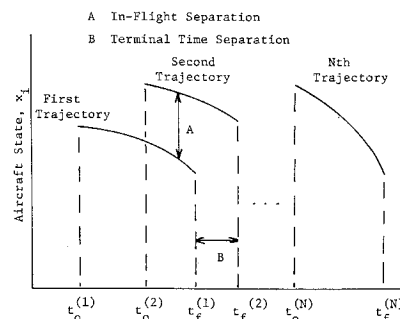


Fig. 2 State history schematic.

Table 1 Initial and final conditions

	CTOL	STOL	Jet transport
Velocity (knots)			
$V_0$	160	225	225
$V_f$	90	60	150
Flight path angle (deg)			
$\gamma_0$	0	0	0
$\gamma_f$	-3	-7.5	-3
Final heading ( $\chi_f$ ) (deg)	180	180	180
Initial range, $R_0$ (naut miles)	20	20	20
Initial azimuth, $\Psi_0$ (deg)	0-(-90)	0-(-90)	0
Initial altitude, $h_0$ (ft)	8000-10,000	8000-10,000	12,000

$a_v$ , the lateral acceleration,  $a_x$ , and the vertical acceleration,  $a_y$ .

The entry conditions for the aircraft arriving into the control zone are considered specified with respect to the terminal area system. In the future, the arrival conditions for all arrivals may be known to the system far before the actual arrival. However, at present, these conditions can only be predicted shortly before arrival. The arrival conditions assumed for the examples to be discussed later are compatible with the assumed vehicle types and current traffic procedures. The aircraft are considered to be in level flight with a velocity-heading-angle directed toward the origin of the ground based coordinate system. The maximum velocity considered at entry was less the requirement for aircraft below 10,000 ft alt in a controlled terminal area. The aircraft could potentially enter at any azimuth angle measured from the runway centerline and at an altitude of, perhaps, between 8000 and 12,000 ft. The formulation and solution technique does not limit these arrival conditions, they are simply chosen as representative for the problem.

The landing gate conditions, or exit conditions, also depend on the type of aircraft being considered. The final approach velocities considered range from 90 knots for slower conventional aircraft, 60 knots for STOL, and 150 knot for large jet transports. The final heading angle is of course aligned with the runway centerline (i.e. in the  $-X$  direction) and the final flight path angle is  $-3^\circ$  for CTOL and  $-7.5^\circ$  for STOL. The exit or landing gate is assumed to be at 2000 ft slant range from the runway threshold and elevated to the proper flight path angle for the particular aircraft. The final 2000 ft before touchdown are not specifically considered in this system. This final portion of the trajectory is fixed since it is assumed the aircraft will require a short, nonmaneuvering final approach to prepare for landing. This requirement is compatible with Farrington<sup>15</sup> in his analysis of autopilot capabilities for a STOL vehicle flying curved terminal-area approaches. For optimum system performance this final gate should be at a minimum distance from the runway threshold, thereby requiring a minimum common flight-path distance.

These terminal conditions result in the following six terminal constraints being imposed on each aircraft trajectory

$$\begin{aligned}
 \psi_1 &= V(t_b) - V_{\text{final}} = 0 & \psi_2 &= \gamma(t_b) - \gamma_{\text{final}} = 0 \\
 \psi_3 &= \chi(t_b) - \Pi = 0 & \psi_4 &= X(t_b) - 2000 \cos |\gamma_{\text{final}}| \\
 \psi_5 &= Y(t_b) = 0 & \psi_6 &= h(t_b) - 2000 \sin |\gamma_{\text{final}}| \quad (6)
 \end{aligned}$$

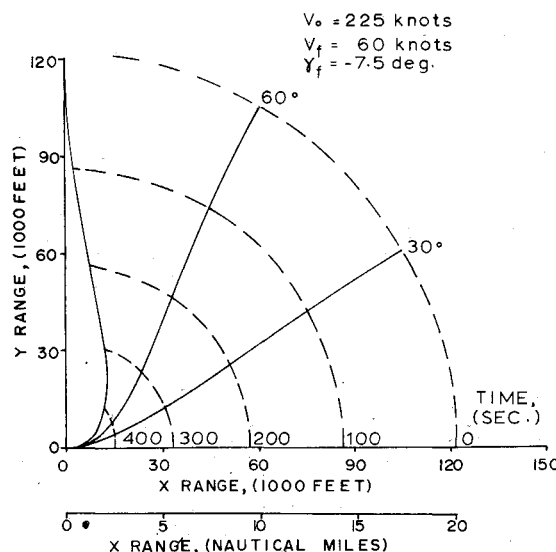


Fig. 3 Time-acceleration optimal trajectories.

### The Steepest-Descent Solution

The flight separation and terminal-time inequality constraints are incorporated into the solution with the use of penalty functions. The terminal-time constraint is treated with a penalty function as described by Kelley<sup>16</sup> which results in an augmented performance index of the form

$$\phi = \phi_0 + K_{t_{ij}} \{ |t_b - t_{b_j}| - \Delta t_{\min} \}^2 \quad (7)$$

In this expression,  $\phi_0$  is the original performance index to be minimized,  $K_{t_{ij}}$  is a nonnegative parameter selected in the solution algorithm, and the remaining term expresses the terminal time constraint. The absolute value of the final time difference implies that the landing order is not initially known.

The flight separation constraint is also treated with a penalty function, but for computational ease the technique of Lasdon, et al.<sup>17</sup> is used. In this approach, the augmented performance index takes the form

$$\phi = \phi_0 + K_{s_{ij}} \int_{t_{a_{ij}}}^{t_b} dt / C(\bar{x}_i, \bar{x}_j) \quad (8)$$

where  $K_{s_{ij}}$  is another non-negative parameter and  $C(\bar{x}_i, \bar{x}_j)$  is the flight-path separation constraint of the form

$$C(\bar{x}_i, \bar{x}_j) = \left\{ \frac{(X_i - X_j)^2 + (Y_i - Y_j)^2}{R_{\min}^2} + \frac{(h_i - h_j)^2}{\Delta h_{\min}^2} \right\}^{1/2} \quad (9)$$

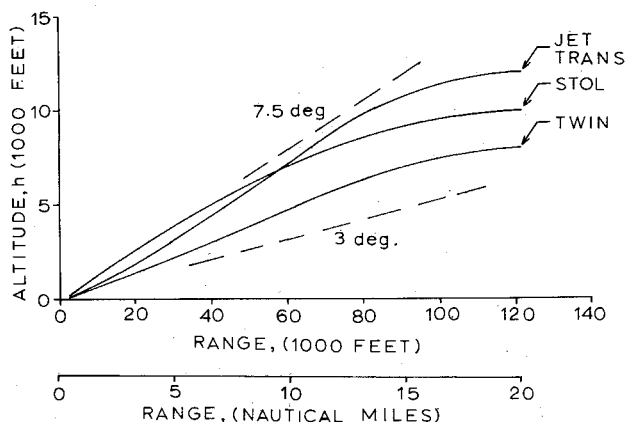


Fig. 4 Time-acceleration optimal flight profiles.

Table 2 Acceleration weighting coefficients

	$w_v$	$w_\gamma$	$w_\chi$
CTOL	3.0	0.1	0.1
STOL	1.0	0.1	0.1
Jet transport	3.0	0.1	0.1

Here  $X_i$ ,  $Y_i$  and  $h_i$  are the position coordinates of aircraft  $i$  and  $R_{\min}$  and  $\Delta h_{\min}$  are the minimum allowable horizontal range and altitude separations, respectively. Clearly this term tends to penalize small aircraft separations and the amount of the penalty will depend on the magnitude of  $K_{sij}$ . It is important to note the definition of the upper and lower limit on the integral,  $t_{aij}$  and  $t_{bij}$ . The integrand is only defined for the time during which aircraft  $i$  and  $j$  are both in the system. Therefore,  $t_{aij}$  is the arrival time of aircraft  $i$  or  $j$ , whichever occurs later, and  $t_{bij}$  is the final time of aircraft  $i$  or  $j$ , whichever occurs earlier. Now the total system index of performance is of the form

$$\begin{aligned} \phi = & \sum_{i=1}^N \{ (t_{bi} - t_{ai}) + \int_{t_{ai}}^{t_{bi}} (\bar{a}_i' W_a \bar{a}_i) dt \} \\ & + \sum_{ij} K_{t_{ij}} \{ |t_{bi} - t_{bj}| - \Delta t_{\min} \}^2 \\ & + \sum_{ij} K_{s_{ij}} \int_{t_{aij}}^{t_{bij}} dt / C(\bar{x}_i, \bar{x}_j) \end{aligned} \quad (10)$$

where, as defined before

- $t_{bi}$  = final time of aircraft  $i$
- $t_{ai}$  = arrival time of aircraft  $i$
- $\bar{a}_i W_a \bar{a}_i$  = weighted acceleration vector squared of aircraft  $i$
- $K_{t_{ij}}, K_{s_{ij}}$  = selected numerical parameters
- $\Delta t_{\min}$  = minimum final time separation
- $C(\bar{x}_i, \bar{x}_j)$  = state-variable position constraint on the flight paths of aircraft  $i$  and  $j$
- $t_{aij}$  = the later of the arrival times of aircraft  $i$  and  $j$
- $t_{bij}$  = the earlier of the final times of aircraft  $i$  and  $j$

and  $\Sigma_{ij}[\cdot]$  represents a sequence of terms  $[\cdot]$ , one for each pair of aircraft  $i, j$ . Consequently, the total unconstrained solution can be initially determined with all the penalty function parameters  $K_{t_{ij}}$  and  $K_{s_{ij}}$  initially set to zero. Then, if a particular separation is violated, the appropriate coefficient is set to a nonzero value. This value is increased until the conflict is eliminated.

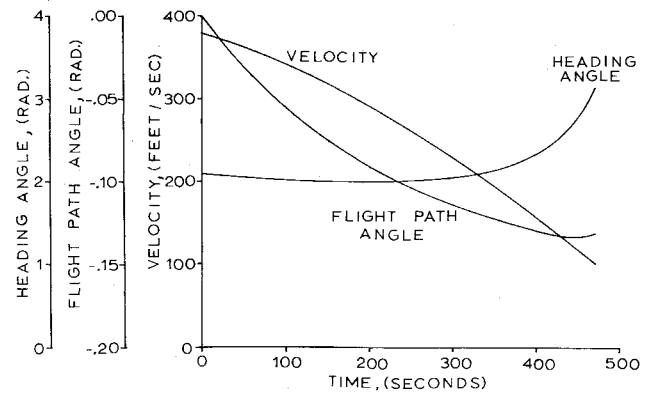
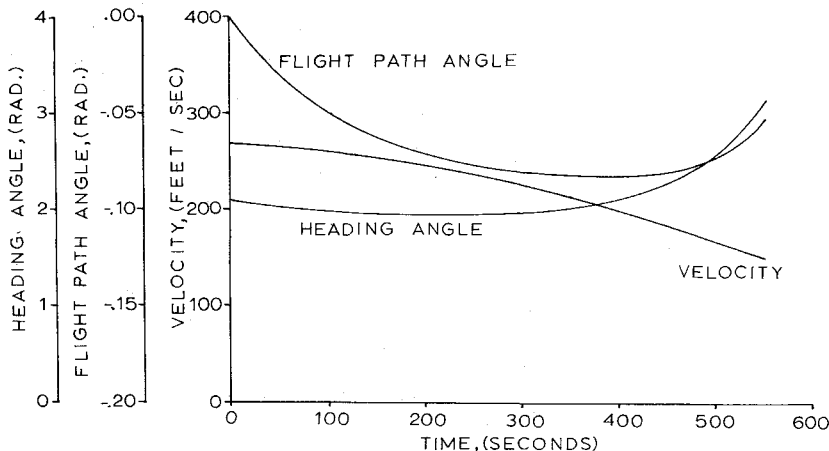


Fig. 5 Velocity, flight path and heading angle histories—STOL.

Now define an auxiliary state variable,  $P_i$ , for each aircraft such that

$$\dot{P}_i = \bar{a}_i' W_a \bar{a}_i \quad (11)$$

and define auxiliary system state variables,  $s_{ij}$ , such that

$$\dot{s}_{ij} = K_{s_{ij}} / C(\bar{x}_i, \bar{x}_j) \equiv g_{ij}(\bar{x}_i, \bar{x}_j) \quad (12)$$

If the initial conditions on these state variables are set to zero and the specified initial times are deleted, the performance index can be stated as

$$\begin{aligned} \phi = & \sum_{i=1}^N \{ t_{bi} + P_i(t_{bi}) \} + \sum_{ij} [ K_{t_{ij}} \{ |t_{bi} - t_{bj}| - \\ & \Delta t_{\min} \}^2 + s_{ij}(t_{bi}) ] \end{aligned} \quad (13)$$

or functionally

$$\phi = \phi \{ \bar{x}_1(t_{b_1}), t_{b_1}, \dots, \bar{x}_N(t_{b_N}), t_{b_N}, \bar{s}(t_{b_s}) \} \quad (14)$$

where the  $\bar{x}_i(t_{b_i})$  are the final values of the state variables of the  $i$ th aircraft, and  $\bar{s}(t_{b_s})$  is the set of all the final values of the system state variables defined by the flight separation penalty functions.

The terminal constraints for each aircraft,  $\bar{\psi}_i$ , involve only the final states of that particular aircraft. Consequently, the adjoint multipliers,  $\bar{\lambda}_{\psi}$ , associated with these terminal constraints are defined by the familiar adjoint equations

$$\dot{\bar{\lambda}}_{\psi} = - \bar{\lambda}_{\psi}' \frac{\partial f_i}{\partial \bar{x}_i} \quad (15)$$

where  $\bar{f}_i$  is defined in the system equations (1). The termi-

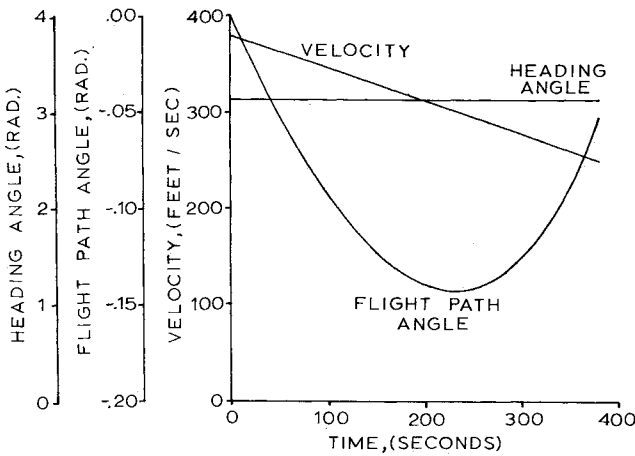


Fig. 7 Velocity, flight path and heading angle histories—jet transport.

nal conditions on the  $\bar{\lambda}_{\psi_i}$ 's are

$$\bar{\lambda}'_{\psi_i}(t_b) = \frac{\partial \psi_i}{\partial \bar{x}_i(t_b)} - \frac{\dot{\psi}_i}{\Omega_i} \frac{\partial \Omega_i}{\partial \bar{x}_i(t_b)} \quad (16)$$

where the stopping condition

$$\Omega_i = \Omega_i(\bar{x}_i(t_b), t_b) \quad (17)$$

is selected from the  $p$  terminal constraints,  $\bar{\psi}_i$ , on the  $i$ th aircraft.

In the case of the performance index

$$I = \phi = \phi\{\bar{x}_1(t_b), t_b, \dots, \bar{x}_N(t_b), t_b, \bar{s}(t_b)\} \quad (18)$$

the analysis is more involved due to the presence of the aircraft and system state variables evaluated at the different terminal times and the different time domains of the system equations. Now the  $i$ th stopping condition,  $\Omega_i$ , determines the final value of the  $i$ th aircraft's state variables. Also, it determines the terminal time for evaluating some of the system separation state variables  $\bar{s}_{ij}(t_{bij})$ . This situation occurs if the  $i$ th aircraft lands before the  $j$ th aircraft (as discussed earlier). When this is the case we will denote  $\Omega_i$  as  $\Omega_{sij}$  even though they are identical.

Now denote the adjoints for each aircraft associated with the performance index as  $\bar{\lambda}_{\phi_i}$  and those associated specifically with the separation constraint auxiliary state variable as  $\bar{\lambda}_{sij}$ . The adjoint equations resulting for these variables are

$$\dot{\bar{\lambda}}_{s_{ij}} = 0 \quad (19)$$

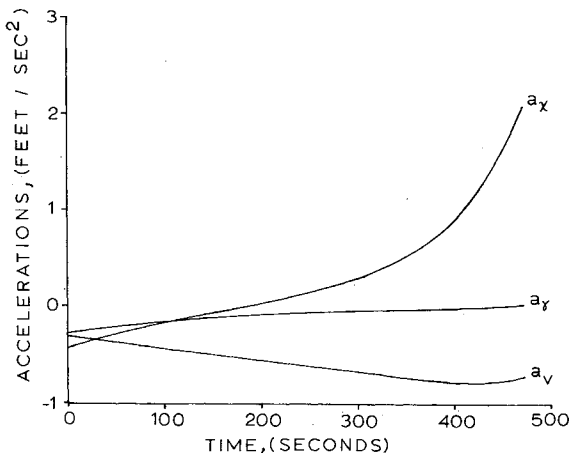


Fig. 8 Acceleration histories—STOL.

Table 3 JET-STOL landing separation summary

	$t_o$ (sec)	$t_{fu}$ (sec)	$W_i A_{iu}^a$	$t_{fc}$ (sec)	$W_i A_{ic}^a$
STOL	0	467	188	512	425
	85	462	138	457	144
Jet	95	472	138	—	482
				482	—

<sup>a</sup>Integral of weighted acceleration quadratic, (ft<sup>2</sup>/sec<sup>4</sup>/sec).

and

$$\dot{\bar{\lambda}}'_{\phi_i} = -\bar{\lambda}'_{\phi_i} \frac{\partial \bar{f}_i}{\partial \bar{x}_i} - U(t - t_a) U(t_b - t) \bar{\lambda}'_{s_{ij}} \frac{\partial \bar{g}_{ij}}{\partial \bar{x}_i} \quad (20)$$

in the interval  $(t_{ai}, t_{bi})$ , where  $\bar{g}_{ij}$  is defined in Eq. (12) and  $U$  is the unit step function defined by

$$U(t - t^*) = \begin{cases} 0 & t < t^* \\ 1 & t \geq t^* \end{cases} \quad (21)$$

The terminal conditions on these adjoints are

$$\begin{aligned} \bar{\lambda}'_{\phi_i}(t_b) &= \frac{\partial \phi}{\partial \bar{x}_i(t_b)} - \frac{\dot{\phi}(i)}{\Omega_i} \frac{\partial \Omega_i}{\partial \bar{x}_i(t_b)} - \frac{\dot{\phi}(s)}{\Omega_{s_{ij}}} \frac{\partial \Omega_{s_{ij}}}{\partial \bar{x}_i(t_b)} \\ \bar{\lambda}'_{s_{ij}}(t_b) &= \frac{\partial \phi}{\partial s_{ij}(t_b)} \end{aligned} \quad (22)$$

where

$$\begin{aligned} \dot{\phi}(i) &= \frac{\partial \phi}{\partial t_b} + \frac{\partial \phi}{\partial \bar{x}_i(t_b)} \dot{\bar{x}}_i(t_b) & \dot{\phi}(s) &= \frac{\partial \phi}{\partial s_{ij}(t_b)} \dot{s}_{ij}(t_b) \\ \dot{\Omega}_i &= \frac{\partial \Omega_i}{\partial t_b} + \frac{\partial \Omega_i}{\partial \bar{x}_i(t_b)} \dot{\bar{x}}_i(t_b) & \dot{\Omega}_{s_{ij}} &= \frac{\partial \Omega_{s_{ij}}}{\partial t_b} + \frac{\partial \Omega_{s_{ij}}}{\partial \bar{x}_i(t_b)} \dot{\bar{x}}_i(t_b) \end{aligned} \quad (23)$$

Note that in Eq. (22), the expression  $\partial \Omega_{s_{ij}} / \partial \bar{x}_i$  is the partial derivative of  $\Omega_{s_{ij}}$  with respect to the states of aircraft  $i$  and is used only if aircraft  $i$  lands first in the aircraft pair  $ij$ .

Now the integral quantities for each trajectory may be defined to be

$$\begin{aligned} I_{\phi\phi_i} &= \int_{t_{ai}}^{t_{bi}} \bar{\lambda}'_{\phi_i} \frac{\partial \bar{f}_i}{\partial \bar{u}_i} W_{u_i}^{-1} \frac{\partial \bar{f}_i}{\partial \bar{u}_i} \bar{\lambda}_{\phi_i} dt \\ I_{\phi\phi} &= \int_{t_{ai}}^{t_{bi}} \bar{\lambda}'_{\phi_i} \frac{\partial \bar{f}_i}{\partial \bar{u}_i} W_{u_i}^{-1} \frac{\partial \bar{f}_i}{\partial \bar{u}_i} \bar{\lambda}_{\phi_i} dt \\ I_{\phi\psi_i} &= \int_{t_{ai}}^{t_{bi}} \bar{\lambda}'_{\phi_i} \frac{\partial \bar{f}_i}{\partial \bar{u}_i} W_{u_i}^{-1} \frac{\partial \bar{f}_i}{\partial \bar{u}_i} \bar{\lambda}_{\psi_i} dt \end{aligned} \quad (24)$$

The  $W_{u_i}$  are selected weighting matrices associated with the control perturbation step size which is

$$dS^2 = \sum_{i=1}^N \int_{t_{ai}}^{t_{bi}} \delta \bar{u}_i' W_{u_i} \delta \bar{u}_i dt \quad (25)$$

The quantities for the system analogous to those for a

Table 4 In-flight separation summary

	$t_o$ (sec)	$t_{fu}$ (sec)	$W_i A_{iu}^a$	$t_{fc}$ (sec)	$W_i A_{ic}^a$
STOL	0	459	179	461	181
Jet	5	382	138	382	139

<sup>a</sup>Integral of weighted acceleration quadratic, (ft<sup>2</sup>/sec<sup>4</sup>/sec).

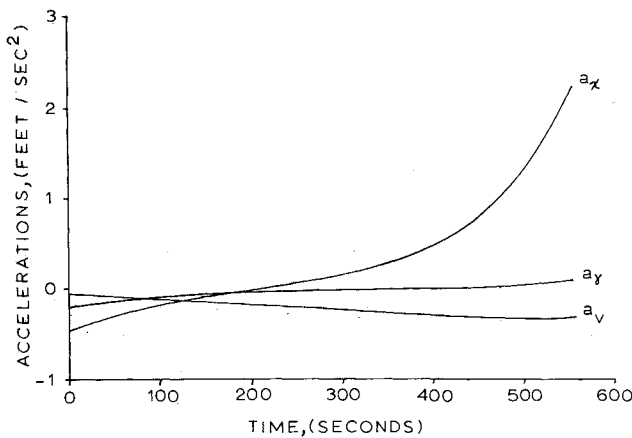


Fig. 9 Acceleration histories—CTOL.

single trajectory can now be defined such that the control perturbations for the  $i$ th aircraft are

$$\delta \bar{u}_i = \pm W_{u_i}^{-1} \left\{ \frac{\partial \bar{f}_i}{\partial \bar{u}_i} \right\} [\bar{\lambda}_{\phi_i} - \bar{\lambda}_{\psi_i} I_{\psi\psi_i}^{-1} I_{\psi\phi_i}] dR + W_{u_i}^{-1} \left\{ \frac{\partial \bar{f}_i}{\partial \bar{u}_i} \right\} \bar{\lambda}_{\psi_i} I_{\psi\psi_i}^{-1} d\bar{\psi}_i \quad (26)$$

where

$$dR^2 = \frac{\sum_{i=1}^N d\bar{\psi}_i' I_{\psi\psi_i}^{-1} d\bar{\psi}_i}{\sum_{i=1}^N \{ I_{\phi\phi_i} - I_{\psi\phi_i}' I_{\psi\psi_i}^{-1} I_{\psi\phi_i} \}} \quad (27)$$

and

$d\bar{\psi}_i$  = desired improvement in the values of  $\psi_i$  for the next iteration (i.e.,  $d\bar{\psi}_i = -K\bar{\psi}_i$ ,  $0 < K < 1$ )

When the  $\bar{\psi}_i$  constraints are met, the gradient of the system performance index with respect to the control perturbation is

$$\frac{d\phi}{dS} = \sum_{i=1}^N \{ I_{\phi\phi_i} - I_{\psi\phi_i}' I_{\psi\psi_i}^{-1} I_{\psi\phi_i} \} \quad (28)$$

The positive sign in Eq. (26) is used if  $\phi$  is to be maximized and the negative sign is used if  $\phi$  is to be minimized.

If all the entry conditions are assumed known in advance, the unconstrained solution for all aircraft is ob-

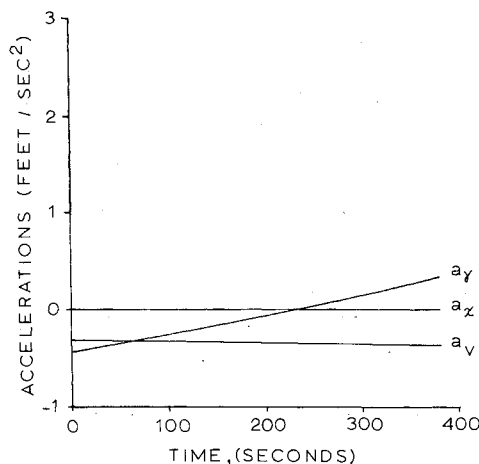


Fig. 10 Acceleration histories—jet transport.

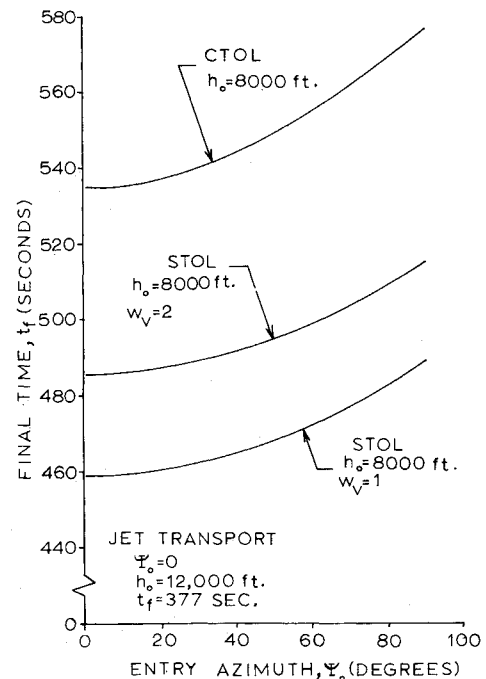


Fig. 11 Parametric final time.

tained first with all the penalty-function coefficients equal to zero. Then, if a separation or terminal-time inequality constraint is violated, the value of the appropriate penalty-function coefficient is increased and the solution is again obtained. This process continues until adequate separations are obtained.

If all aircraft's initial conditions are not initially known, a sequential solution algorithm is used. For example, assume the entry conditions for an aircraft are made known to the "system" one minute before its arrival. The solution for this aircraft may then be obtained prior to its arrival time. Then, at some time later, a second entering aircraft's entry conditions are "reported" one minute before it's arrival. Now, while the first aircraft follows its initially prescribed trajectory and prior to the second aircraft arrival, this two-aircraft solution may be obtained. If no conflict between the two aircraft occurs, the initial aircraft's trajectory will not be perturbed. In the case of a conflict, both aircraft's initial trajectories will be constrained to alleviate it. However, for an algorithm of this type to operate in real time, the average time required for solution must be less than the interarrival rate of the aircraft.

### Example Results

With curved approaches and a minimal use of common flight paths, it is conceivable that in many instances a

Table 5 Three aircraft solution summary

	Solution one	Solution two
	Init. cond. known	Sequential algorithm
Final time (sec):		
CTOL	605	602
STOL	546	544
Jet	488	486
Integrated accelerations (ft <sup>2</sup> /sec <sup>4</sup> /sec):		
CTOL	84	93
STOL	173	178
Jet	156	160
Performance index	2052	2063

particular aircraft may not violate the separation criteria with another. Also, even if such encounters do occur, the unconstrained solutions are required to determine the landing sequence. Consequently, parametric results have been obtained for some independent aircraft examples. Three aircraft categories are considered with different speed ranges and different entry and exit conditions. These are presented in Table 1.

The emphasis in these examples will be on cases in which the slower, more maneuverable aircraft (e.g. light twins and STOLs) will approach the landing gate from the side, while the larger jet transports will follow a more "straight-in" approach. Consequently, the entry azimuth for the jet transport will always be zero.

The weighting matrix for the acceleration in the performance index was taken as a diagonal matrix. The diagonal elements for the three aircraft categories are given in Table 2.

The weighting on the longitudinal acceleration,  $w_v$ , is smaller on the STOL than on the other two to reflect the fact that STOL aircraft will usually exhibit greater longitudinal controllability through the use of larger flap deflections or jet-tilt devices. Also, the weighting on the lateral accelerations and vertical accelerations,  $w_x$  and  $w_y$ , is less than on the longitudinal accelerations. This also is due to the greater controllability in these axes than along the longitudinal direction.

The horizontal ground traces for a STOL-type aircraft entering at 10,000 ft alt are parametrically given in Fig. 3 to show the geometry of the trajectories for various entry azimuths. The trajectories for a CTOL-type craft result in a geometry varying only slightly from that given. The altitude-range profiles for the three aircraft categories are then given in Fig. 4. The entry azimuth for the jet is zero while that for the other aircraft is  $-60^\circ$ . These profiles are quite insensitive to entry azimuth when plotted versus ground range,  $R$ . For reference, the velocity, flight-path and heading-angle histories for these three trajectories are given in Figs. 5-7. The acceleration histories are then given in Figs. 8-10. The final times for the aircraft are given parametrically versus entry azimuth in Fig. 11, while the integrated accelerations are shown in Fig. 12.

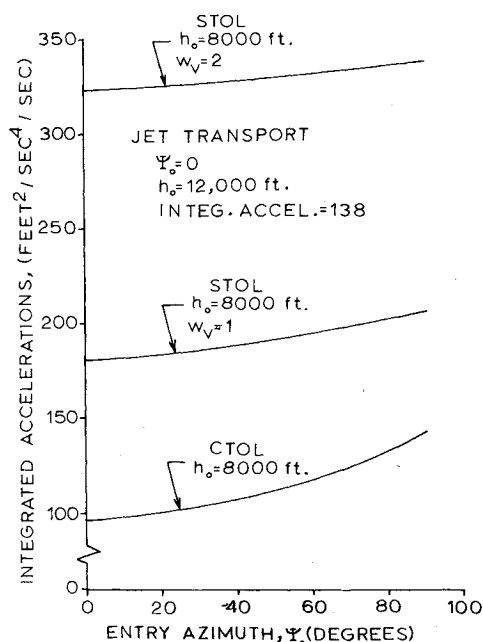


Fig. 12 Parametric integrated accelerations.

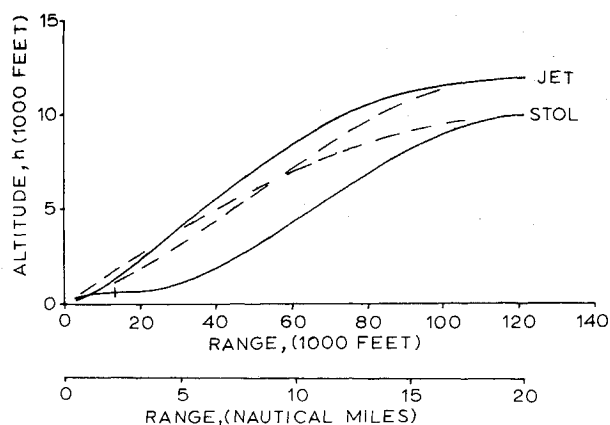


Fig. 13 Jet-STOL air separation flight profiles.

Also depicted in these figures is the effect of doubling the longitudinal acceleration weighting coefficient for the STOL aircraft.

An example involving conflicts between two aircraft at the terminal time includes a STOL aircraft entering at an azimuth of  $-45^\circ$ , 10,000 ft altitude and a jet transport following a straight approach entering at 12,000 ft. The unconstrained final time for the STOL is 467 sec after entry, while that for the jet is 377 sec after entry. Consequently, if a jet arrives 90 sec after a STOL vehicle, a conflict will occur at the final gate. Table 3 summarizes the results for two examples of this type. In the first case the jet enters 85 sec after the STOL and lands first, while in the second case, the jet enters 95 sec after the STOL and lands second. The resulting final times and integrated accelerations for the aircraft are given. The solution algorithm requires the landing sequence in the constrained case to be the same as the sequence when unconstrained. Upon further investigation, this assumption was found to lead to a sub-optimal solution for the jet arriving at 95 sec (i.e. the landing order should actually be reversed). The minimum final time separation required is 60 sec ( $\pm 5$  sec). When this time separation was achieved, the 1.5 naut mile horizontal range and 1000 ft alt separation criteria were not violated.

An example involving only an in-flight separation conflict involves a STOL vehicle and a jet, both entering at an azimuth of zero. The jet arrives at an altitude of 12,000 ft while the STOL arrives at 10,000 ft. This results in the unconstrained trajectories crossing at approximately 10 miles from the runway threshold, as shown in Fig. 4. If the jet arrives 5 sec after the STOL, this crossing occurs at the same time along the trajectories, thereby violating the in-flight separation constraint. The resulting constrained trajectories are given in Fig. 13, with the dashed lines showing the unconstrained trajectories. The tick mark near the end of the STOL trajectory shows the position of this vehicle when the jet arrives at the landing gate. The final times and integrated accelerations are summarized in Table 4. The final time separation is greater than 60 sec in both the constrained and unconstrained cases.

The final example involves three aircraft, one of each type. The CTOL vehicle is assumed to arrive at an azimuth of  $-45^\circ$  and an altitude of 8000 ft. A STOL vehicle also arrives at  $-45^\circ$  azimuth and 10,000 ft alt. Finally, a jet arrives at zero azimuth and 12,000 ft alt. The assumed arrival time of the CTOL is taken as a zero reference time. The STOL enters one minute later, while the jet arrives another minute later, after the STOL. This results in the unconstrained landing times of 547, 527 and 497 sec for the CTOL, STOL and jet, respectively. Two solutions for this case were obtained. The first assumed the entry

conditions were all known and the entire three-aircraft problem was solved. The second solution assumed the initial conditions were only known one minute before the respective aircraft's arrival. This second solution then involved three problems, the single aircraft solution for the CTOL, then the CTOL-STOL two-aircraft solution, and finally, the three aircraft solution. This entire sequential solution was obtained in one computation "run." When one solution was obtained, the initial conditions for the "new" aircraft were then input while the initial conditions for the aircraft already in the "system" were updated to those one minute later (in simulated time) along their previously prescribed trajectory. This portion of the solution was then obtained. The final times and total integrated accelerations for the two solution techniques are summarized in Table 5. The difference in the final performance indices reflects the penalty due to the lack of knowledge of the entry conditions before the entire multi-aircraft problem is solved.

### Summary

The formulation and an example solution technique has been presented for the determination of the landing sequence and multiple-aircraft flight paths which lead to the minimization of the sum of the aircraft flight durations and integrated accelerations in the terminal area. The formulation is based on the theory of disconnected optimal trajectories, while the Steepest-Descent technique is used for obtaining the solutions to some example problems. Terminal time and in-flight separation inequality constraints are imposed and penalty functions were used. This effort is intended to be a step toward the ultimate goal of automated terminal area trajectory and landing sequence specification.

For an approach of this type to operate on-line, alternate solution techniques and computational hardware must be investigated. The Steepest-Descent approach, although helpful in obtaining preliminary results, lacks the speed and reliability for on-line usage. For these examples the computation time required (on the CDC 6500 machine) ranged from 40 sec for a single trajectory to 265 sec for a three-aircraft example. The sequential solution of the last example discussed required 45 sec for the initial single-aircraft trajectory, 95 sec more for the two-aircraft solution and 170 additional sec for the final solution involving the three aircraft. Faster computational hardware and/or software or perhaps even hybrid computation may possibly provide the necessary speed for on-line operation. Alternatively, simpler algorithms for quickly obtaining semi-optimal results would also be adequate.

Another approach, potentially even more attractive, could make use of precomputed trajectories and sequencing policies. These could be stored parametrically and thus the complete two-point-boundary-value problems need not be calculated over and over for each aircraft.

The computer-controller need only "interpolate" between precomputed trajectories and control policies.

### References

- <sup>1</sup>"Report of the Department of Transportation Air Traffic Control Advisory Committee," Vols. I and II, Dec. 1969, Dept. of Transportation, Washington, D.C.
- <sup>2</sup>Schmidt, D. K., "Optimal Multiple Aircraft Control for Terminal Area Approach," Ph.D. dissertation, Dec. 1972, School of Aeronautics, Astronautics, and Engineering Sciences, Purdue University, West Lafayette, Ind.
- <sup>3</sup>Blumstein, A., "An Analytical Investigation of Airport Capacity," Rept. TA-1358-G-1, 1960, Cornell Aeronautical Lab., Buffalo, N.Y.
- <sup>4</sup>Simpson, R. W., "Analytical Methods of Research into Terminal Area Air Traffic Operations," *Journal of Aircraft*, Vol. 2, No. 3, May-June 1965, pp. 185-193.
- <sup>5</sup>Telson, M. L., "An Approach to Optimal Air Traffic Control During the Landing Phase," M.S. thesis, Dept. of Electrical Engineering, 1969, M.I.T., Cambridge, Mass.
- <sup>6</sup>Athans, M. and Porter, L. W., "An Approach to Semi-Automated Scheduling and Holding Strategies for Air Traffic Control," 1971 *Joint Automatic Control Conference Preprints*, August 11-13, 1971, pp. 536-545.
- <sup>7</sup>Tobias, L., "Automated Aircraft Scheduling Methods in the Near Terminal Area," *Journal of Aircraft*, Vol. 9, No. 8, Aug. 1972, pp. 520-524.
- <sup>8</sup>Cherry, G. W., DeWolf, B., and MacKinnon, D., "Increasing Airport Capacity and Terminal Area Safety by Means of the Scanning Beam Instrument Landing System," AIAA Paper 70-1033, Santa Barbara, Calif., 1970.
- <sup>9</sup>Erzberger, H. and Lee, H. Q., "Optimal Horizontal Guidance Techniques for Aircraft," *Journal of Aircraft*, Vol. 8, No. 2, Feb. 1971, p. 95.
- <sup>10</sup>Lee, H. Q. and McLean, J. D., "Guidance Technique for Automated Air Traffic Control," AIAA Paper 72-121, San Diego, Calif., 1972.
- <sup>11</sup>Shultz, R. L. and Kilpatrick, P. S., "Aircraft Optimum Multiple Flight Path," JANAIR Rept. 700709, June 1970, Honeywell Inc., Minneapolis, Minn.
- <sup>12</sup>Vincent, T. L. and Mason, J. D., "Disconnected Optimal Trajectories," *Journal of Optimization Theory and Applications*, Vol. 3, No. 4, April 1969, pp. 263-281.
- <sup>13</sup>Mason, J. D., "Some Optimal Branched Trajectories," CR-1331, May 1969, NASA.
- <sup>14</sup>Denham, W. F., "Steepest-Descent Solution of Optimal Programming Problem," Harvard Summer Program on Optimization of Dynamic System, July 22-Aug. 2, 1963, Raytheon Co., Bedford, Mass.
- <sup>15</sup>Farrington, F. D. and Goodson, R. E., "Simulation of a STOL Aircraft with Digital Autopilot on a Curved Approach with Scanning Beam Microwave Guidance," Jan. 1972, Automatic Control Center, School of Mechanical Engineering, Purdue University, West Lafayette, Ind.
- <sup>16</sup>Kelley, H. J., Falco, M., and Ball, D. J., "Air Vehicle Trajectory Optimization," Symposium on Multivariable Systems Theory, Nov. 1962, Soc. Indust. and Applied Mathematics, Cambridge, Mass.
- <sup>17</sup>Lasdon, L. S., Warren, H. D., and Rice, R. K., "An Interior Penalty Method for Inequality Constrained Optimal Control Problems," *Transactions of the IEEE on Automatic Control*, Vol. AC-12, Aug. 1967, pp. 388-395.